RSC Advances

PAPER

View Article Online
View Journal | View Issue

Cite this: *RSC Adv.*, 2015, **5**, 37721

Green fabrication of 3-dimensional flower-shaped zinc glycerolate and ZnO microstructures for *p*-nitrophenol sensing†

Apurba Sinhamahapatra, Dhrubajyoti Bhattacharjya and Jong-Sung Yu*

Received 8th April 2015
Accepted 17th April 2015

DOI: 10.1039/c5ra06286a

www.rsc.org/advances

The solvent or reaction medium always plays a lead role in synthesis chemistry. Glycerol has been studied as a green solvent for different organic transformations and is also expected to give interesting control in material synthesis. In this study, we use aqueous glycerol to synthesize zinc glycerolate and the corresponding ZnO micro-flower structures with an intention to encourage the utilization of glycerol as a green reaction medium in material synthesis. A zinc ammonium complex is used as a source of zinc, which converts to zinc glycerolate in the presence of glycerol. Glycerol plays a dual role as a reactant to form zinc glycerolate and as a solvent to control the morphology. The unreacted glycerol is recovered after the reaction and reused further. The flower-structured zinc glycerolate and ZnO are then used for the first time to modify a glassy carbon electrode to make a binder-free non-enzymatic amperometric chemical sensor for *p*-nitrophenol that is a brutal environmental pollutant. The modified electrode is found to be an excellent alternative for the purpose with respect to sensitivity, selectivity and stability.

Introduction

The solvent plays pivotal roles in deciding the chemical structure as well as morphology of the final product during material preparation.[1–9] It also determines the post reaction factors, like choice of work-up procedures, recycling or disposal strategies. On the other hand, a large amount of solvent used for chemical process is a big threat to the environment. Considering the environmental legislation, the search for green solvents has been the most important and challenging task for researchers recently.[1,2] However, material chemists are comparatively less concerned about the use of green solvent although water, supercritical CO_2 and ionic liquids are commonly used as green solvents in material preparations.[1,2]

In this regard, glycerol can be good choice as green solvent.[1,3,10] Nowadays, the use of glycerol has already gained interest in organic synthesis due to its unique properties like remarkable solubility, very high boiling point (290 °C), low vapor pressure.[1,3–6,10,11] In addition, glycerol is nontoxic, biodegradable, non-flammable, safe to use and largely available, which make it greener and sustainable solvent in comparison to other organic solvents and polyol (*e.g.* ethylene glycol) that are often used in material chemistry. Therefore, use of glycerol as solvent is an interesting area of research and attracting more attention to develop greener protocols for material synthesis. Glycerol also shows good chelating behavior towards transition metal which can add further interest to the synthesis of materials with controlled morphology.

Here, it should be also mentioned that the research on the utilization of glycerol is also provoked by the continuous growing demand of biodiesel in modern days as it is a major side product obtained during production of biodiesel. In fact, almost 1 kg of glycerol is generated during preparation of ~10 kg of biodiesel.[10]

In recent days, besides organic synthesis, the use of glycerol also started in material synthesis as a novel solvent system. One of the important recognized uses of glycerol in material chemistry is synthesis of metal nanoparticles with high purity.[1] High purity Cu, Ag, Au, Pt and Pd nanoparticles were synthesized in glycerol with high yield.[12–14] Interestingly, glycerol also acts as a reducing agent. Further, different nanostructured materials were synthesized using glycerol in the presence of co-solvent like water, ethanol or any nonpolar solvent.[6,15–26] Co-solvent also plays an important role when glycerol is used as solvent. Not only plummeting the viscosity of glycerol, but it also helps to form emulsion which has a definite impact on the morphology of the final product.[24] Glycerol was also used as a medium for synthesis of polypyrrole nanospheres and carbon dots.[27–29]

Department of Energy Systems Engineering, Daegu Gyeongbuk Institute of Science & Technology (DGIST), Daegu, 711-873, Republic of Korea. E-mail: jsyu@dgist.ac.kr; Fax: +82-53-785-6409; Tel: +82-53-785-6443

† Electronic supplementary information (ESI) available: Comparison of present and earlier reported methodology of zinc glycerolate prepared with different synthesis conditions, synthesis condition in details, thermal analysis, probable chemical reactions involved during synthesis of materials and results of temperature dependency, interference and stability study of the modified electrode. See DOI: 10.1039/c5ra06286a

In this context, we would like to report the use of glycerol–water as a green solvent for the fabrication of novel flower-like zinc glycerolate and corresponding zinc oxide (ZnO) microstructures from zinc ammonium complex in reflux method. Present study also recognizes glycerol–water system as greener reaction medium for material synthesis which is rarely discussed before. The study also discusses role of water and glycerol for the formation of flower-like morphology. The reusability of the glycerol is also studied as one of the key features of green solvent. Successful reuse in the present work has special meaning as the reuse of glycerol for material synthesis rarely been approached earlier. ZnO is a potential and commonly studied n-type semiconductor having a large band gap of 3.37 eV. It has been investigated for wide range of applications such as in sensors, piezoelectric and photoelectric devices, solar cells, light emitting diodes and catalysis.[29] Due to its applicability and unique properties, fabrication of nanoscale ZnO is all time favorite area of research and several shapes for nanoscale ZnO have been introduced.[24,28–34] However, three-dimensional (3D) hierarchical assembled porous structures are always gaining some special attention due to some specific applications like sensors, lithium-ion batteries, solar cells and catalysis.[29,30] Therefore, development of new synthetic methodology for 3D nanostructured ZnO is always desired. Additionally, zinc glycerolate is also an important compound in bio-medical field. It is one of the important slow-release nontoxic sources of therapeutic zinc with antiarthritic, antiulcer, and antiinflammatory activities.[35] Recently, zinc glycerolate was also found to play as heterogeneous catalyst for the synthesis of fatty acid methyl esters and formation of glycerol carbonate.[36,37]

Here, it should be mentioned that polyol-mediated synthesis of ZnO was reported earlier.[25,26,36–42] However, these reports have rarely discussed the sustainability of the develop protocols and also often used glycol or poly glycol as solvent which is more hazardous compared to glycerol. Furthermore, most reports on synthesis on zinc glycerolate and corresponding ZnO with different morphology did not recognized the use of glycerol as green medium for material synthesis.[25,35,38–40] One of the main intension of the present work is to establish and point out glycerol as an efficient green solvent system for synthesis of materials with controlled morphology. It is also noticed that the earlier process affords specified morphology of zinc glycerolate at much higher temperature and differs from the present developed methodology in respect of synthesis conditions (Table S1, ESI†).

Furthermore, the synthesized flower-shaped zinc glycerolate and ZnO microstructures are used to make binder-free glassy carbon electrode (GCE), which can be used as an electrochemical sensor for *p*-nitrophenol (PNP). Nitrophenols are found in both terrestrial and aquatic environments and considered as serious environmental contaminants, which are mainly comes from the industrial sectors like pesticides, dyes, and pharmaceuticals.[43–50] Convulsion, cyanosis, coma, and even death for human beings can happen on contact to these compounds by inhalation, ingestion, eye or skin.[43,44] These are mostly highly toxic in nature, highly soluble in water, showing carcinogenicity, remain for a long time in environment and are very difficult to degrade.[43] Among these, PNP is the most atrocious and listed as priority pollutant by the United States Environmental Protection Agency (USEPA). Therefore, it is highly desired to develop efficient, reliable, robust and highly sensitive sensor for the detection of PNP.[50] In this study, the synthesized zinc glycerolate and corresponding ZnO flower structures are used to modify glassy carbon electrode (GCE) for PNP sensing for the first time.

Experimental

Materials

All the chemicals were obtained from either Sigma-Aldrich or Samchun chemicals (South Korea) and used as received.

Synthesis of flower shaped zinc glycerolate and ZnO microstructure

In a typical procedure, 0.3 mM of zinc nitrate was dissolved in 20 ml water, and excess amount of 30% (v/v) ammonium hydroxide was added drop-wise with continuous stirring to get a clear solution of metal ammonium complex (pH $\sim$ 9). 40 ml of glycerol was added to the clear solution and stirred for 30 min. The final solution was either stirred at room temperature or refluxed or kept in autoclaved at 100 °C for 12 h. After that, a white precipitate was obtained, which was filtered and washed thoroughly with water and ethanol. The material was dried at 80 °C for 12 h to afford flower-shaped zinc glycerolate, and on subsequent calcination at 500 °C for 4 h in aerobic condition, ZnO was obtained with identical morphology. The as-synthesized zinc glycerolate samples are denoted as ZG-X (where X = 1, 2, 3.....). To study the formation of flower shape, the synthesis was performed in different time intervals, keeping other parameters constant.

Characterization

The Scanning Electron Microscope (SEM) images of the synthesized zinc glycerolate and zinc oxide samples were obtained using Hitachi Scanning Electron Microscope (SEM) S-4700, operated at an acceleration voltage of 10 kV. Transmission Electron Microscopy (TEM) images were collected using JEOL FE-2010, operated at 200 kV. Powder X-ray diffraction (XRD) data were recorded using a Rigaku Smartlab diffractometer with Cu-Kα (0.15406 nm) operated at 40 kV and 30 mA at a scan rate of 4° min^{-1}. The nitrogen adsorption–desorption isotherms of the samples were measured at −196 °C using a Micromeritics ASAP 2460 accelerated surface area and porosity analyzer after the samples were degassed at 150 °C to 20 mTorr for 12 h. The specific surface area was determined based on Brunauer–Emmett–Teller (BET) method from nitrogen adsorption data in the relative pressure range from 0.05 to 0.2. Pore size distribution was derived from desorption branches by the Barrett–Joyner–Halenda (BJH) method. Thermal Gravimetric Analysis (TGA) was carried out on a Bruker TG-DTA3000SA thermal analyzer at a heating rate of 10 °C min^{-1} under flowing N_2, increasing from room temperature to 600 °C to investigate the decomposition of zinc glycerolate materials.

Fabrication of modified electrode for PNP sensing and electrochemical measurements

For the detection of PNP, glassy carbon electrode (GCE) having surface area 0.0707 cm^2 was modified with resultant nanostructured materials and the modified electrode was designated as sample name/GCE. Before modification, the surface of GCE was polished with 0.05 μm alumina slurry followed by rinsing with water thoroughly, and dried at room temperature. 5.0 mg of flower-shaped ZnO was dispersed in 1.0 ml water and sonicated for 10 min. 5 μl of suspension was dropped on the cleaned GCE surface and dried at room temperature for 24 h. All the electrochemical experiments were performed at room temperature with a conventional three-electrode system, which consists of modified GCE as a working electrode, a Pt wire as a counter electrode and a Ag/AgCl (saturated KCl) electrode as a reference electrode, using an electrochemical workstation (VMP3, Biologic) in phosphate buffer solution (PBS) of pH 7.

Results and discussion

Synthesis and characterization of the materials

In the present study, glycerol–water was used as a reaction medium for the synthesis of flower-shaped zinc glycerolate and ZnO with an aim to encourage the utilization of glycerol for the fabrication of nanostructured materials as a green solvent. The previous studies,[15–28,36–41] which uses glycerol as solvent for material synthesis, rarely explore or deliberate it as a green reaction medium for nanostructured material synthesis. Besides, as a reaction medium, glycerol also acts as a reagent to form zinc glycerolate in this work. A clear solution of zinc ammonium complex was prepared from $Zn(NO_3)\cdot 6H_2O$ and ammonium hydroxide and used as a source of zinc. The freshly prepared clear solution of zinc ammonium complex was mixed with water–glycerol mixture and kept in different conditions to obtain a white precipitate of zinc glycerolate which produced ZnO on subsequent calcination.

Different experiments are designed by varying the parameters to synthesize zinc glycerolate. SEM images of different synthesized zinc glycerolate microstructures are represented in the Fig. 1 and specific reaction conditions with obtained morphology are summarized in Table S2 (ESI†). At the earlier stage, three different sets of reaction were performed using simple stirring at room temperature, reflux and solvothermal treatment at 100 °C, respectively with other parameters and reactant concentration kept the same. The respective samples are ZG-1, ZG-2 and ZG-3. Short rod-like structures without any definite 3D morphology were obtained at room temperature, while nice flower-like morphology with uniform size and shape was observed for the sample synthesized by reflux condition. In solvothermal condition, comparatively bigger and compact flower-like morphology was obtained. It looks like rod-like primary structures assemble to form flower-like morphology upon increasing the reaction temperature. So, to obtain definite 3D controlled morphology of zinc glycerolate from zinc ammonium complex and glycerol, it seems that temperature (100 °C) treatment is necessary. Here, it should be mentioned

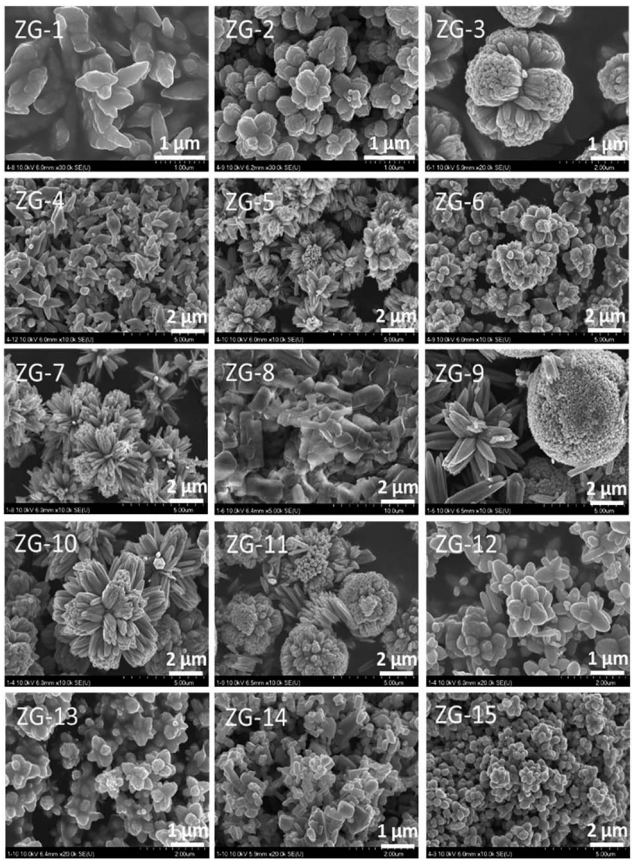

Fig. 1 SEM images of synthesized zinc glycerolate microstructures.

that the required temperature is comparatively lower than that of the previously reported process.[25,35,38–40] Besides, it was also observed that the yield of obtained material was quite low for the synthesis performed at room temperature.

After that, different samples were synthesized by varying the ratio of glycerol and water using reflux (ZG-2, ZG-4, ZG-5, ZG-6, ZG-7) and solvothermal (ZG-3, ZG-8, ZG-9, ZG-10, ZG-11) treatments. The SEM images of the synthesized materials clearly show that different definite 3D flower-like morphologies are obtained with different ratios of glycerol and water in reflux condition. Only the sample ZG-2 and ZG-6 look somewhat similar with uniform flower-structure. This dissimilarity in morphology of the synthesized samples proves the dependency of glycerol–water ratio. It can be also realized that glycerol and water both influences on the obtained morphology. In case of solvothermal synthesis, somewhat different 3D morphologies are also observed with different glycerol water ratios. However, uniform definite morphology is obtained only for the sample ZG-3 and ZG-10. These used the same ratios (glycerol : water ratios of 1 : 0.5 and 1 : 1) that were used for ZG-2 and ZG-6, respectively. These results clearly indicate that for the present study, the above mentioned ratio of glycerol and water is able to produce uniform definite 3D flower morphology of zinc glycerolate. It also suggests that in the present case, reflux condition is comparatively better than solvothermal treatment. Further study was carried out using different zinc sources like $ZnCl_2$,

$Zn(O_2CCH_3)_2(H_2O)_2$ and ZnO instead of $Zn(NO_3)\cdot 6H_2O$ in reflux condition. The study reveals that with other zinc salt, somewhat deformed flower like morphology (ZG-12, ZG-13) was obtained, or no specified uniform morphology was observed from ZnO (ZG-14). This suggests that the presence of other anions in the system during the formation of material has some influence on the final morphology of materials. The presence of different anions may influence the formation of zinc glycerol complex and consequently final morphology of the obtained materials. This can be strongly supported by no specified morphology obtained when ZnO is used as starting material as there is no extra anion (like, NO_3–, Cl– or CH_3 COO–) present in the system.

The powder X-ray diffraction (XRD) patterns of ZG-2 and calcined ZG-2 are presented in Fig. 2a. The bottom XRD pattern reveals specific characteristic peaks of zinc glycerolate for the sample before calcination. The characteristic diffraction peaks at $2\theta = 10.9°$, 20.67°, 17.12°, and 27.53° can be indexed to (1 0 0), (1 1 1), (0 0 1) and (2 1 1), respectively, according to the ICDD no. 23-1975. This strongly suggests the formation of zinc mono glycerolate ($Zn(C_3H_6O_3)$). Relative high intensity of the signal at $2\theta = 10.9°$ also suggest crystallographic preferred orientation along [1 0 0] axis.[36] This phenomenon can be correlated to directional growth of petals for formation of flower-like microstructure as seen in SEM image. To obtain the flower-shaped ZnO, zinc glycerolate precursor was calcined at 500 °C for 4 h in aerobic condition. The powder XRD pattern of the calcined material shows formation of ZnO with pure zincite phase of hexagonal system (ICDD no. 36-1451). The well-resolved peaks with high intensity are indexed to (1 0 0), (0 0 2), (1 0 2), (1 0 1), (1 0 2), (1 1 0), (1 0 3), (2 0 0), (1 1 2), (2 0 1), (0 0 4), and (2 0 2) planes of the hexagonal structure of ZnO. No peaks corresponding to impurities like zinc hydroxide and zinc glycerolate are observed, which indicates the formation of pure ZnO crystal phase. The SEM image of calcined ZG-2 material is presented in Fig. 2b. It is clearly observed that the flower morphology is retained after calcination, but the flower is more opened up in comparison to zinc glycerolate structure. This phenomenon can be stated as the blooming of flowers. The zinc glycerolate (ZG-2) was further characterized by TGA (Fig. S1, ESI†). The observed weight loss (~47%) in the temperature range of 280 to 480 °C is attributed to the removal of chemically bonded glycerol moiety. The differential thermal gravimetric (DTG) analysis shows a peak at 383 °C. This value confirms the formation of zinc monoglycerolate.[36]

The corresponding TEM images of the calcined ZG-2 sample are presented in Fig. 3, while TEM image of corresponding ZG-2 precursor is represented in the inset of Fig. 3a. The low resolution TEM image (Fig. 3a) of calcined ZG-2 shows the flower-shaped morphology resembling the corresponding SEM image in Fig. 2b. The arrangement of petals are clearly perceptible in higher resolution image (Fig. 3b). It also indicates that the petals are single crystalline rather consist of smaller crystallite, which further proved by the continuous lattice fringe observed in the petals (Fig. S2, ESI†). Presence of distinct lattice fringes in the high-resolution TEM image confirms high crystallinity of ZnO structure. The lattice fringe spacing of 0.26 nm is in good agreement with the *d*-spacing between the (0 0 2) planes of hexagonal wurtzite ZnO (Fig. 3c) in support of XRD pattern. The selected area electron diffraction ring pattern indicates polycrystalline nature of the ZnO flower (Fig. 3d).

The N_2 adsorption–desorption analysis of ZG-2 and calcined ZG-2 samples results in BET surface areas of 1.3 and 27 $m^2\ g^{-1}$, respectively. The low surface area of zinc glycerolate was also previously reported and this may be due to the presence of organic species and low porosity. During heat treatment in aerobic condition, the huge weight loss occurs due to glycerol decomposition to CO_2 to produce ZnO and the flower structure is more opened up like blossoming of flowers as observed in TEM (Fig. 3a) and SEM (Fig. 2b) image which leads to higher surface area. This phenomena can be supported by observed hysteresis loop in the N_2 isotherms with desorption average pore width ($4V/A$) of 5.3 nm (the isotherm figure not shown).

To understand the formation of above presented flower-shaped morphology in glycerol–water medium, SEM analysis was carried out for different samples obtained in different

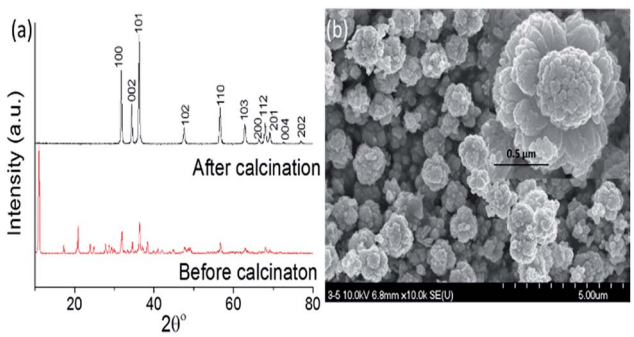

Fig. 2 (a) Powder XRD patterns of ZG-2 and calcined ZG-2 and (b) SEM image of calcined ZG-2.

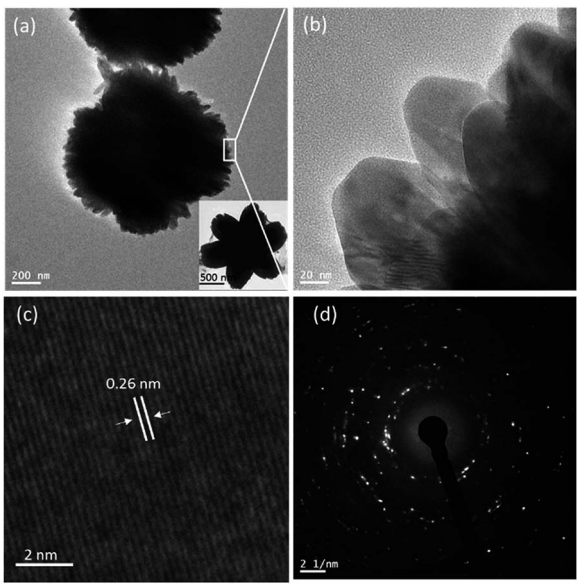

Fig. 3 TEM images of calcined ZG-2 (a and b) and TEM image of ZG-2 (inset of (a)). Lattice fringe pattern (c) and electron diffraction pattern (d) of calcined ZG-2.

reaction times with maintenance of reaction parameters used in sample ZG-2 except reaction time. Based on the different SEM images obtained for zinc glycerolate, a pictorial diagram of step by step formation path is represented in Fig. 4 for the corresponding flower-shaped morphology. As depicted in Fig. 4, the clear solution of zinc ammonium complex in aqueous glycerol becomes turbid within 0.2 to 0.3 h. No specified morphology is observed at this stage. It looks like small pieces of amorphous bean-like sludge. In the next stage around 1 h of reaction, the growth in different directions of the bean-shaped structure is observed, just like petals oriented in different directions of a flower, which gradually turns into the final flower-shaped morphology of zinc glycerolate due to crystallographically preferred orientation growth in around twelve hour of reaction. The nucleation and growth can be resembled to the La Mer concept.[51] At the initial stage, the clear solution of zinc ammonium complex releases ammonia on heating and produces Zn^{2+} ion, which further reacts with glycerol to produce zinc glycerolate. The concentration of zinc glycerolate is increased steadily with time and form a nuclei *via* homogeneous self-nucleation as concentration reached to supersaturation levels. With continuous supply of monomers, the nuclei grow in a preferred direction to form the petals of the flowers in glycerol medium. The directional growth to form petals can be supported by the XRD pattern of zinc glycerolate (Fig. 2a) and its single crystalline nature as observed in the HR-TEM analysis (Fig. 3 and S2, ESI†). On calcination in air, the ZnO flower structure is more opened up.

To understand the role of glycerol, the present adopted synthesis method is analyzed step by step by chemical reactions involved (Scheme S1, ESI†). In the first step, zinc nitrate and ammonium hydroxide produces a clear solution of zinc tetra-ammonium complex. After that, the clear solution was added to aqueous glycerol. On heating, the zinc tetra-ammonium complex produces the mono zinc glycerolate due to ligand exchange reaction with the release of ammonia gas, and a solid product starts to be generated, which produces ZnO upon calcination. The formation of mono zinc glycerolate complex is confirmed by the XRD result of the as-synthesized material.

Here, it should be mentioned that the present nitrate ions may participate in stabilization/destabilization process of different metal complexes involved during synthesis and also help in the formation of final morphology as discussed earlier.

Reusability is the one of the important features of green solvent. The reuse of glycerol as solvent for material synthesis has been rarely approached earlier. Here, it should be mentioned, although glycerol is one of the reactants to form zinc glycerolate but it is also used as a solvent to obtain the present flower-like morphology. So, we have tried to reuse the used glycerol as solvent for further synthesis. For this, after collection of the white precipitate by filtration, the filtrate was collected, and the water was removed from the mixture using a rotary-evaporator. The water-free glycerol was then again used for synthesis of ZG-2 sample following the same procedure and as expected, identical morphology was obtained as shown in the SEM image of ZG-15 in Fig. 1. The recovered glycerol also was analyzed by 1-H NMR spectroscopy, and no significant change was observed. It shows only glycerol protons, and the spectrum was similar to commercial pure glycerol that was used in this study.

Application of the synthesized materials

As a result, interesting 3D flower-shaped zinc glycerolate and corresponding ZnO are successfully fabricated using aqueous glycerol. The synthesized flower-shaped zinc glycerolate (ZG-2) and corresponding ZnO were further investigated for the fabrication of electrode to sense PNP electrochemically. The samples were dispersed in water and drop-casted on the clean surface of GCE to achieve binder-free modified electrodes. The modified GCE was studied as PNP amperometric chemical sensor in PBS of pH 7 using cyclic voltammetry. The obtained cyclic voltammograms in presence and absence of PNP are presented in Fig. 5.

In Fig. 5a, presented CVs were recorded in absence of PNP. It is clearly seen that modified electrode ZnO/GCE shows highest current compared to ZG-2/GCE and bare GCE, indicating that modification of GCE improves the performance. Representative

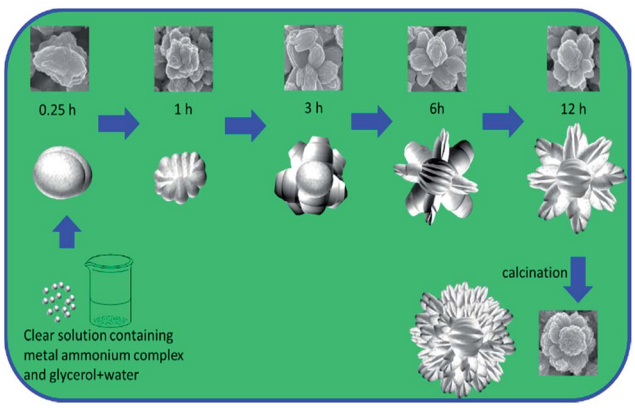

Fig. 4 Schematic representation for step-wise formation of flower-shaped zinc glycerolate and corresponding ZnO microstructure.

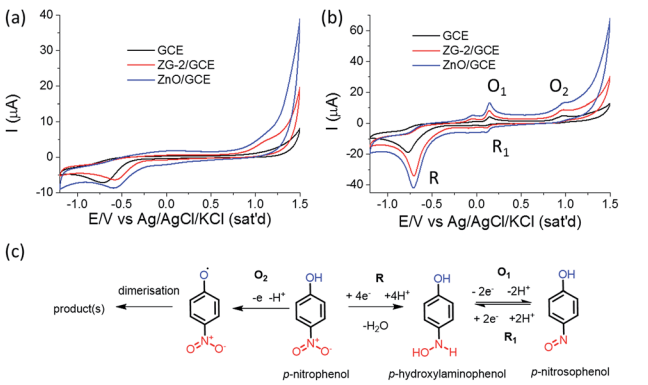

Fig. 5 CVs of bare GCE and modified GCEs (a) in the absence and (b) in the presence of 0.5 mM of PNP in PBS of pH 7 at a scan rate of 50 mV s^{-1}. (c) Probable electrochemical redox reactions involved for PNP sensing.

CVs of different electrodes in the presence of 0.5 mM PNP in Fig. 5b clearly show the difference in the current trend, similar to the results in the absence of PNP, but with much higher current response and new signals upon addition of PNP. The CVs taken in the presence of PNP also clearly exhibit a new irreversible reduction peak (R) around −0.74 V and a pair of new reversible oxidation (O_1) and reduction (R_1) peak observed at around 0.145 V and 0.113 V, respectively for the electrode modified by the developed flower-shaped ZnO microstructure (ZnO/GCE). The obtained results are similar to previously reported results using α-MnO_2 nanotube modified GCE.[44] The responses towards PNP of synthesized zinc glycerolate and ZnO-modified GCE are quite impressive and make them promising candidates for the amperometric electrochemical PNP sensor. ZnO shows better performance compared to zinc glycerolate as ZnO is a semiconductor and possesses electron communication ability, which leads to higher current response.[43] The probable electrochemical redox reactions[44] taking place during sensing are presented in Fig. 5c. The first step is irreversible reduction (R) of *p*-nitrophenol to *p*-hydroxyaminophenol with involvement of 4 electrons and release of one water molecule. The next step is reversible 2-electron redox (O_1 and R_1) transformation in between *p*-hydroxyaminophenol and *p*-nitrosophenol. Here, it should be mentioned that a further oxidation (O_2) of phenolic group to a radical species is also occurred, and the irreversible oxidation peak around 1.1 V can be attributed to this phenomenon.[52,53]

The performance of ZnO/GCE-modified electrode is further studied in different scan rates from 10 to 500 mV s^{-1} in the presence of 0.5 mM PNP, and the CVs are presented in Fig. 6a. The values of peak current corresponding to oxidation and reduction, increase linearly with the increasing scan rate and exhibit a linear relation with the root of scan rate (Fig. 6a inset). The peak potential difference (ΔE_p) is founded ~45 mV which is higher than the expected value (59/2 mV) for a perfectly reversible reaction. This phenomenon indicated that the electrochemical reaction at electrode surface is quasi-reversible reaction. However, there is no significant change observed in the peak potential difference (ΔE_p) with respect to the scan rate.

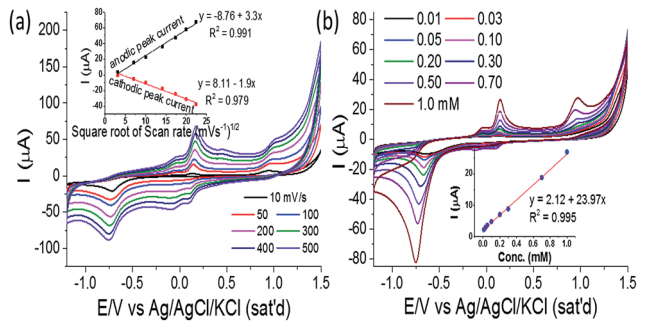

Fig. 6 CVs obtained (a) in different scan rates (inset: plots of O_1 peak current and R_1 peak current *vs.* square root of scan rate with linear fitting) and (b) in the presence of different PNP concentrations at 50 mV s^{-1} scan rate (inset: plot of O_1 peak current *vs.* PNP concentration with linear fitting) for ZnO/GCE.

The observation clearly indicates that the reaction of PNP over the modified electrode is a diffusion-controlled process. Further, the modified electrode is studied for PNP detection as a function of temperature (Fig. S3, ESI†). The CVs at different temperatures show that the current response of oxidation peak O_1 and O_2 increases with the decrease of oxidation potential upon increase of temperature. This phenomenon indicated faster oxidation reaction at high temperature. The irreversible reduction peak (R) current also increases similarly, whereas the reversible R_1 peak current decreases with increasing temperature. The phenomena indicate the decrease of reversibility by accelerating the oxidation step (O_1) and decelerating the reversible (R_1) step with the increase of temperature.

To further understand the PNP sensing performance, the developed flower-shaped ZnO-modified electrode is subjected to different concentrations of PNP from 0.01 mM to 1.0 mM and CV is recorded in Fig. 6b. From the series of CVs presented in Fig. 6b, it is clearly seen that peak currents of the corresponding redox reaction are increasing with the increase of PNP concentration. The Fig. 6b inset shows the linear relationship of the peak current of O_1 peak with PNP concentration with a correlation coefficient of 0.994. This observation can be the clear evidence of that the present modified electrode ZnO/GCE can detect PNP in the linear range of 0.01 to 1 mM. The sensitivity is 404.35 μA mM^{-1} cm^{-2}, and LOD (limit of detection) is calculated to be 0.013 mM considering initial four points with a correlation coefficient of 0.994. Here, it should be mentioned that on further increase in PNP concentration beyond 1.0 mM, no further increase in current response of O_1 peak is observed and the linear relation between current and concentration (Fig. S4, ESI†) also destroyed (Fig. S5, ESI†). The R_1 peak position also shifted towards lower potential with large decrease in current response. This phenomenon may indicate surface contamination of the modified electrode due to continuous decomposition of PNP.

On further investigation, the performance of ZnO/GCE electrode is studied in the presence of different interferents, and no significant influence is found in the current of O_1 peak (Fig. S6a, ESI†), demonstrating remarkable selectivity towards PNP in presence of similar nitrophenol derivatives. The stability of the fabricated electrode is also studied and the results are presented in Fig. S6b (ESI†). It is founded that the peak current value of O_1 peak is decreased gradually after each consecutive usage for 7 days, and after 1 month, it still maintains around 60% of initial peak current. Interestingly, 95% of peak current is observed for O_1 peak when the electrode is stored without use.

For comparative study, the commercial nanocrystalline ZnO (surface area = 11 m^2 g^{-1}, no definite morphology and size, Fig. S7, ESI†) was also used to modify GCE and studied for PNP detection under the same conditions. The results show lower current response (O_1 Peak) than that of the present synthesized flower-shaped ZnO (Fig. S8, ESI†). The enhancement of the current responses can be attributed to the enhanced electron exchange ability of well-interconnected networks formed by the 3D flower-shaped ZnO and higher surface area of flower-shaped ZnO compared to commercial random-shaped nanocrystalline ZnO. The above results for the present fabricated electrode ZnO/

GCE are quite impressive compared to the previously reported GCE-based modified electrodes[44–48] for PNP sensing, and thus, the present ZnO/GCE can be a promising alternative.

Conclusions

In conclusion, flower-shaped zinc glycerolate microstructures were synthesized using aqueous glycerol as a green reaction medium for the first time from zinc ammonium complex. Zinc ammonium complex afforded zinc glycerolate micro-flower in the presence glycerol at 100 °C, which is relatively lower temperature than that of earlier reports. Corresponding ZnO was obtained upon calcination in aerobic condition. The glycerol–water ratio has influence on the final morphology. The glycerol can be easily recovered and it can be used again. So the present process is simple, economical and sustainable to achieve zinc glycerolate and ZnO microstructures. The synthesized flower-shaped zinc glycerolate and ZnO microstructures were used for the fabrication of amperometric electrochemical PNP sensor for the first time. The modified electrode showed promising results for PNP sensing with high selectivity and relatively long-term stability and can be an excellent candidate for the determination PNP in polluted water. Thus, glycerol as green medium for material synthesis can find more attention in future to develop a sustainable chemical process for safe environment. In addition, developed zinc glycerolate and ZnO-based sensors can also find interest for monitoring other environmental pollutants in sustainable way for the healthy environment.

Acknowledgements

The work was supported by NRF grant (NRF-2010-0029245) and Global Frontier R&D Program at Center for Multiscale Energy System (NRF-2011-0031571) funded by Korean government. Authors also thank KBSI at Jeonju and Daejeon for SEM and TEM measurements.

Notes and references

1 Y. Gu and F. Jérôme, *Green Chem.*, 2010, **12**, 1127–1138.
2 Y. Medina-Gonzalez, S. Camy and J.-S. Condoret, *ACS Sustainable Chem. Eng.*, 2014, **2**, 2623–2636.
3 A. E. Díaz-Álvarez and V. Cadierno, *Appl. Sci.*, 2013, **3**, 55–69.
4 J. H. Kim, D. Bhattacharjya and J.-S. Yu, *J. Mater. Chem. A*, 2014, **2**, 11472–11479.
5 W. Yanga, Z. Gaoa, J. Maa, J. Wanga, B. Wanga and L. Liu, *Electrochim. Acta*, 2013, **112**, 378–385.
6 B. Fang, N. K. Chaudhari, M.-S. Kim, J. H. Kim and J.-S. Yu, *J. Am. Chem. Soc.*, 2009, **131**, 15330–15338.
7 N. K. Chaudhari, H. C. Kim, C. S. Kim, J. Park and J.-S. Yu, *CrystEngComm*, 2012, **14**, 2024–2031.
8 N. K. Chaudhari, S. Chaudhari and J.-S. Yu, *ChemSusChem*, 2014, **7**, 3102–3111.
9 N. K. Chaudhari, M.-S. Kim, T.-S. Bae and J.-S. Yu, *Electrochim. Acta*, 2013, **114**, 60–67.
10 J. I. García, H. García-Marín and E. Pires, *Green Chem.*, 2014, **16**, 1007–1010.
11 G. Cravotto, L. Orio, E. C. Gaudino, K. Martina and D. Tavor, *ChemSusChem*, 2011, **4**, 1130–1134.
12 A. Sinha and B. P. Sharma, *Mater. Res. Bull.*, 2002, **37**, 407–416.
13 A. Sinha and B. P. Sharma, *Bull. Mater. Sci.*, 2005, **28**, 213–217.
14 J. Kou, C. Bennett-Stamper and R. S. Varma, *ACS Sustainable Chem. Eng.*, 2013, **1**, 810–816.
15 G. Galgali, E. Schlangen and S. van der Zwaag, *Mater. Res. Bull.*, 2011, **46**, 2445–2449.
16 J. Yin and H. Cao, *Inorg. Chem.*, 2012, **51**, 6529–6536.
17 Z. Zhang, J. Hao, W. Yang, B. Lu, X. Ke, B. Zhang and J. Tang, *ACS Appl. Mater. Interfaces*, 2013, **5**, 3809–3815.
18 S. Chen, F. Liu, Q. Xiang, X. Feng and G. Qiu, *Electrochim. Acta*, 2013, **106**, 360–371.
19 Y. Li, X. Yan, W. Yan, X. Lai, N. Li, Y. Chi, Y. Wei and X. Li, *Chem. Eng. J.*, 2013, **232**, 356–363.
20 H. Li, Z. Bian, J. Zhu, D. Zhang, G. Li, Y. Huo, H. Li and Y. Lu, *J. Am. Chem. Soc.*, 2007, **129**, 8406–8407.
21 A. Escudero, E. Moretti and M. Ocañaa, *CrystEngComm*, 2014, **16**, 3274–3283.
22 Z. Ma, G. Shao, Y. Fan, G. Wang, J. Song and T. Liu, *ACS Appl. Mater. Interfaces*, 2014, **6**, 9236–9244.
23 Y. Yan, Z. Zhou, Y. Cheng, L. Qiu, C. Gao and J. Zhou, *J. Alloys Compd.*, 2014, **605**, 102–108.
24 B. Wang, J. S. Chen, H. B. Wu, Z. Wang and X. W. Lou, *J. Am. Chem. Soc.*, 2011, **133**, 17146–17148.
25 S. Zhang, P. Yang, A. Zhang, R. Shi and Y. Zhu, *CrystEngComm*, 2013, **15**, 9090–9096.
26 R. Moleski, E. Leontidis and F. Krumeich, *J. Colloid Interface Sci.*, 2006, **302**, 246–253.
27 F. Ghamouss, A. Brugère, A. C. Anbalagan, B. Schmaltz, E. Luais and F. Tran-Van, *Synth. Met.*, 2013, **168**, 9–15.
28 L.-H. Mao, W.-Q. Tang, Z.-Y. Deng, S.-S. Liu, C.-F. Wang and S. Chen, *Ind. Eng. Chem. Res.*, 2014, **53**, 6417–6425.
29 S. K. Arya, S. Sahab, J. E. Ramirez-Vickc, V. Guptab, S. Bhansali and S. P. Singhe, *Anal. Chim. Acta*, 2012, **737**, 1–21.
30 A. Sinhamahapatra, A. K. Giri, P. Pal, S. K. Pahari, H. C. Bajaj and A. B. Panda, *J. Mater. Chem.*, 2012, **22**, 17227–17235.
31 A. K. Giri, A. Sinhamahapatra, S. Prakash, J. Chaudhari, V. K. Shahi and A. B. Panda, *J. Mater. Chem. A*, 2013, **1**, 814–822.
32 S. G. Kumar and K. S. R. Koteswara Rao, *RSC Adv.*, 2015, **5**, 3306–3351.
33 P.-P. Wang, Q. Qi, R.-F. Xuan, J. Zhao, L.-J. Zhoua and G.-D. Li, *RSC Adv.*, 2013, **3**, 19853–19856.
34 X. Dong, Y. Cao, J. Wang, M. B. Chan-Park, L. Wang, W. Huanga and P. Chen, *RSC Adv.*, 2012, **2**, 4364–4369.
35 R. Rémiás, Á. Kukovecz, M. Darányi, G. Kozma, S. Varga, Z. Kónya and I. Kiricsi, *Eur. J. Inorg. Chem.*, 2009, 3622–3627.
36 M. Reinoso, D. E. Damiani and G. M. Tonetto, *Appl. Catal., B*, 2014, **144**, 308–316.
37 T. W. Turney, A. Patti, W. Gates, U. Shaheena and S. Kulasegaram, *Green Chem.*, 2013, **15**, 1925–1931.

38 H. Dong and C. Feldmann, *J. Alloys Compd.*, 2012, **513**, 125–129.
39 A. Mezni, F. Kouki, S. Romdhane, B. Warot-Fonrose, S. Joulié, A. Mlayah and L. S. Smiri, *Mater. Lett.*, 2012, **86**, 153–156.
40 N. Mira, M. S. Niasaria and F. Davarc, *Chem. Eng. J.*, 2012, **181–182**, 779–789.
41 I. Trenque, S. Mornet, E. Duguet and M. Gaudon, *Inorg. Chem.*, 2013, **52**, 12811–12817.
42 B. W. Chieng and Y. Y. Loo, *Mater. Lett.*, 2012, **73**, 78–82.
43 F. Karim and A. N. M. Fakhruddin, *Rev Environ Sci Biotechnol*, 2012, **11**, 261–274.
44 J. Wu, Q. Wang, A. Umar, S. Sun, L. Huang, J. Wanga and Y. Gao, *New J. Chem.*, 2014, **38**, 4420–4426.
45 Y. Xu, Y. Wang, Y. Ding, L. Luo, X. Liu and Y. Zhang, *J. Appl. Electrochem.*, 2013, **43**, 679–687.
46 Y. Tang, R. Huang, C. Liu, S. Yang, Z. Lua and S. Luo, *Anal. Methods*, 2013, **5**, 5508–5514.
47 M. A. El Mhammedi, M. Achak, M. Bakasse and A. Chtainia, *J. Hazard. Mater.*, 2009, **163**, 323–328.
48 G. Bharath, V. Veeramani, S.-M. Chen, R. Madhu, M. M. Raja, A. Balamurugan, D. Mangalaraj, C. Viswanathan and N. Ponpandian, *RSC Adv.*, 2015, **5**, 13392–13401.
49 R. Panigrahia and S. K. Srivastava, *RSC Adv.*, 2013, **3**, 7808–7815.
50 M. M. Rahman, G. Gruner, M. S. Al-Ghamdi, M. A. Daous, S. B. Khan and A. M. Asiri, *Chem. Cent. J.*, 2013, **7:60**, 1–12.
51 V. K. LaMer and R. H. Dinegar, *J. Am. Chem. Soc.*, 1950, **72**, 4847–4854.
52 T. Alizadeha, M. R. Ganjalib, P. Norouzib, M. Zareb and A. Zeraatkar, *Talanta*, 2009, **79**, 1197–1203.
53 K. C. Honeychurch and J. P. Hart, *Electroanalysis*, 2007, **19**, 2176–2184.